

## Chain model for the spiral instability of the force-free configuration in thin superconducting films

Yu. A. Genenko

*Institut für Materialphysik, Universität Göttingen, Hospitalstrasse 3-7, D-37073, Göttingen, Germany  
and Donetsk Physical & Technical Institute of the National Academy of Sciences of Ukraine, 340114 Donetsk, Ukraine*

P. Troche and J. Hoffmann

*Institut für Materialphysik, Universität Göttingen, Hospitalstrasse 3-7, D-37073, Göttingen, Germany*

H. C. Freyhardt

*Institut für Materialphysik, Universität Göttingen, Hospitalstrasse 3-7, D-37073, Göttingen, Germany  
and Zentrum für Funktionswerkstoffe gGmbH, Windausweg 2, D-37073, Göttingen, Germany*

(Received 26 May 1998)

The developed stage of a spiral instability of the magnetic flux line in a thin film is studied. The instability of a one-dimensional (1D) flux-line lattice parallel to a thin superconducting film surface and to a transport current is modeled as a transformation of initial linear flux lines into chains of 2D vortices crossing the film and tilted in the field direction. The pitch length of the first instable spiral-like chain structure turns out to be of the order of a film thickness at all fields, which leads to a dissipation rate comparable in magnitude with the experimental one. [S0163-1829(98)08941-3]

### I. INTRODUCTION

The resistive behavior of a current-carrying type-II superconductor subjected to a longitudinal magnetic field is still poorly understood theoretically<sup>1</sup> and far from being completely documented experimentally. In this configuration, usually called “force-free,”<sup>2</sup> the transport current exerts no (Lorentz) force upon flux lines (FL’s) parallel to its direction. Thus, the theoretical problem is to comprehend the reasons for a flux motion and energy dissipation in this case, in other words, the mechanism of resistivity, which is still disputable.<sup>3</sup>

Experimentally, the longitudinal resistivity exhibits a rather specific behavior. Typical of this are the enhancement of a critical current in a parallel field<sup>4</sup> and the onset of a considerable longitudinal magnetic moment (depending on the current applied) in a small or even zero external field.<sup>2,5,6</sup> An interesting feature of this state is the appearance of the regular<sup>5,6</sup> or stochastic<sup>7</sup> oscillations of the longitudinal magnetic moment and voltage.

Assuming a steady-state electric field in a current direction requires a continuous flow of a transverse component of a magnetic field in a sample. It was comprehended that such a flow may be provided by the entry of inward-collapsing right-handed spiral vortices following the pattern of a stray field.<sup>2</sup> But this process leads to a continuous buildup of a longitudinal magnetic flux in the sample.<sup>8</sup>

A principal solution to circumvent this dilemma was suggested by Clem<sup>9</sup> who discovered in 1977 an instability of a single flux line in a current-carrying superconductor against certain left-handed helical perturbations provided the current is sufficiently high. Thus, the longitudinal resistivity may be caused by a succession of right-handed helices entering and left-handed helices leaving the sample (both events contribute to the positive longitudinal electric field). Above the

characteristic current of instability, various types of dissipation cycles become possible.<sup>9-13</sup>

Following the pioneering work of Clem,<sup>9</sup> Brandt considered a more realistic case of the helical instability of a flux-line lattice (FLL) (Ref. 10) in fields  $H \gg H_{c1}$ , the field of the first magnetic vortex penetration in the bulk sample. He found that a critical current of a homogeneous helical distortion of the FLL is equal to zero in the pin-free case: e.g., the force-free configuration is absolutely instable in an ideal bulk superconductor, though, thanks to the very large typical wavelength of this instability (of the order of sample length), even a very weak pinning may stabilize the FLL.<sup>11</sup> Later on, comprehensive models for a steady-state dissipation in a longitudinal field were advanced by Clem<sup>12</sup> and Brandt<sup>13</sup> who explained the onset of a longitudinal paramagnetic moment and gave reasonable values for the oscillation frequency of some shuttle process of the flux entry and exit. The problem which remained unsolved was an extremely low dissipation rate proportional to  $(\xi/R)^2$ , where  $\xi$  is the superconducting coherence length and  $R$  is a transverse size of a sample, which was many orders less than voltage oscillations observed in experiment.<sup>6</sup>

To study in detail the local mechanism triggering the spiral instability and look for regimes yielding a higher energy dissipation, the low-dimensional case of a thin superconducting film carrying a transport current parallel to an external magnetic field may be considered. Theoretically, it is favorable because the process of FLL formation in the increasing magnetic field is well studied in films at all stages: from well-separated single FL’s to a one-dimensional FLL and then to a few-layer FLL.<sup>14-16</sup>

The nucleation of a left-handed instability in thin films was considered in Ref. 17 where the characteristic current of instability was found to be of the order of the critical currents observed in thin films. The threshold characteristic field of the instability turned out to be close to the first critical field

of FL penetration into the film,  $H_{c1}(d)$ ,<sup>14</sup> where  $d$  is the thickness of the film.

To obtain the dissipation rate in thin films one should consider the further development of the growing left-handed spiral and, for the realistic case of a field well above the  $H_{c1}(d)$ , take into account the interaction with the other FL's. Finally, the steady-state dissipation cycle regime of the sort of a "shuttle process" considered by Clem<sup>12</sup> should be advanced to explain the resistivity in the longitudinal geometry.

For these aims, a model of a spiral instability in films is advanced in this paper, based on the idea of the transformation of the growing left-handed spiral into a chain of tilted vortices crossing the film. Section II contains a qualitative description of the model and the calculation of a single flux-line instability valid for an external field slightly above  $H_{c1}(d)$ . In Sec. III we consider the instability of a one-dimensional (1D) FLL valid for a field well above  $H_{c1}(d)$  and estimate the resistivity following from the corresponding "shuttle process." The results are summarized in Sec. IV.

## II. CHAIN INSTABILITY OF A SINGLE FLUX LINE

### A. Qualitative description of the model

A basic reason for the instability of a magnetic FL parallel to a transport current is the Lorentz force applied upon the FL element and proportional to the vector product  $\mathbf{j} \times \mathbf{n}$  where  $\mathbf{j}$  is a local density of the transport current and  $\mathbf{n}$  is the tangent vector of the FL. As was noticed by Clem,<sup>9</sup> in the case of a left-handed spiral distortion of FL's this force acts outwards (contrary to the right-hand case) against the line tension and the Meissner-current-mediated force from the external field. If the transport current is large enough, the linear FL parallel to it becomes unstable and transforms in a growing left-handed helical spiral. This process in thin films was studied in Ref. 17 for the nucleation stage only when the radius of the helix  $r \ll d \ll \lambda$  and  $L$ , where  $\lambda$  and  $L$  are the magnetic field penetration depth and pitch length of the spiral, respectively.

What happens, then, when the spiral diameter  $2r$  first attains the thickness of the film  $d$ ? The circular cross section of the spiral FL should be first distorted due to the attraction to mirror images in the upper and lower film surfaces and then the vortex would cross the surface of the film as is shown in Fig. 1(a). It is likely from energy reasons<sup>18,19</sup> that, at low fields, a spiral-like structure which follows from this crossing process may hardly be formed by long (on the scale of  $d$ ) strongly tilted vortices [shown by a dashed line in Fig. 1(b)] but rather by well-separated 2D vortices tilted with respect to a normal to the surface in a field direction [solid lines in Fig. 1(b)]. The further development of this spiral-like structure formed by the two chains of vortices directed up and down, respectively, as is shown in Fig. 1(c), proceeds as a movement of the chains driven by the Lorentz force in opposite directions (outwards). By this motion, the tilt angle of the vortices may also change.

For symmetry reasons, the vortices in the left and right chains are equally tilted with respect to the external field (and current) direction that coincides with positive  $y$  axis direction. To evaluate the energy of the structure and estimate the dissipation rate during its expansion one should first

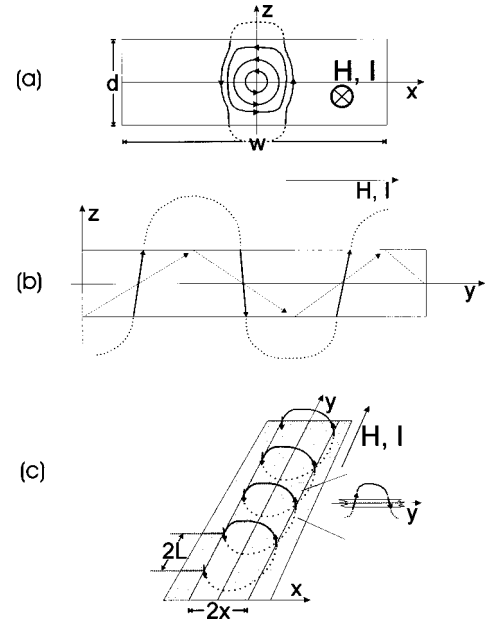


FIG. 1. (a) A cross section of a growing left-handed spiral: first round (helix), then distorted by the attraction to a film surface, (b) a spiral-like structure formed by strong tilted (dashed) or slightly tilted (solid) vortices, and (c) two vortex chains resulting from the development of a helical spiral.

calculate the field of the arbitrary tilted vortex and the energy of interaction between the tilted vortices.

### B. Field of a tilted vortex

We continue now with a calculation of the magnetic field induced by an individual tilted vortex in a thin film. This problem was considered before mostly as a problem of a tilted FLL in fields well above  $H_{c1}$ .<sup>18-21</sup> On the other hand, considering the straight tilted vortex crossing a thin film we do not need in general the complicated expressions obtained in Ref. 19 for an arbitrary curved single vortex in a plate of arbitrary thickness. In what follows, we directly calculate the magnetic field distribution in the London approach assuming the case of a strong type-II superconductor with  $\lambda \gg \xi$  and field range  $H \ll H_{c2}$ , where  $H_{c2}$  is the upper critical field of the superconductor.

We consider a superconducting film of thickness  $d$  and width  $W$  satisfying the inequalities  $\xi \ll d \ll \lambda$  and  $W \gg \Lambda = \lambda^2/d \gg \lambda$  where  $\Lambda$  is a transverse penetration depth for films.<sup>22</sup> The film occupies the region  $|z| \leq d/2$ ,  $|x| \leq W/2$  and is infinite along the  $y$  axis. The magnetic field of the vortex alone,  $\mathbf{h}$ , obeys inside the superconductor the London equation

$$\lambda^2 \text{curl curl } \mathbf{h} + \mathbf{h} = \Phi \quad (1)$$

and the Maxwell equation

$$\text{div } \mathbf{h} = 0, \quad (2)$$

where the source function on the right-hand side (RHS) of Eq. (1) is given by<sup>23</sup>

$$\Phi = \Phi_0 \int d\mathbf{l} \delta(\mathbf{r} - \mathbf{l}). \quad (3)$$

$\Phi_0$  is the unit flux quantum,  $\delta(\mathbf{r})$  the three-dimensional delta function,  $\mathbf{l}$  the position vector of the vortex singularity, and  $d\mathbf{l}$  the flux-line element. The integration goes along the flux line (vortex core).

Outside the superconductor,  $\mathbf{h}$  obeys the Maxwell equations

$$\text{curl } \mathbf{h} = 0, \quad \text{div } \mathbf{h} = 0 \quad (4)$$

and is continuous in all components at the film boundaries  $|z| = d/2$  and vanishes as  $|x|$ ,  $|y|$  or  $|z| \rightarrow \infty$ .

Since the vortices in thin films are straight and slightly tilted even for field directions close to the film surface,<sup>18,19,24</sup> we consider further a straight vortex line tilted for simplicity only along the  $y$  axis and parametrized by the coordinate  $z$  as

$$l_x = R_x, \quad l_y = R_y + kz, \quad l_z = z. \quad (5)$$

Here the vector  $\mathbf{R}$  denotes the point of the vortex crossing the symmetry plane of the film at  $z=0$ . The two-dimensional vector  $\mathbf{k}$  has the same direction as the projection of the vortex line on the plane  $z=0$  and is equal to  $\tan \beta$ , where  $\beta$  is the tilt angle with respect to the perpendicular direction to the film [see Fig. 2(a)]. In this case, the line integration in Eq. (3) may be performed explicitly and gives the following expressions for the components of the vector  $\Phi$ :

$$\Phi^x = 0, \quad \Phi^y = k\Phi_0 \delta(x - R_x) \delta(y - R_y - kz),$$

$$\Phi^z = \Phi_0 \delta(x - R_x) \delta(y - R_y - kz). \quad (6)$$

It is convenient to solve Eqs. (1), (2), and (4) with the help of a Fourier transformation

$$\mathbf{h} = \int \frac{d^2 \mathbf{q}}{(2\pi)^2} \mathbf{h}_{\mathbf{q}}(z) \exp(i\mathbf{q} \cdot \mathbf{s})$$

where  $\mathbf{s} = (x, y)$  denotes the two-dimensional position vector. In these terms the functions (6) are reduced to

$$\Phi_{\mathbf{q}}^x = 0, \quad \Phi_{\mathbf{q}}^y = k\Phi_0 \exp(-i\mathbf{q} \cdot \mathbf{R} - i\mathbf{k} \cdot \mathbf{q}z),$$

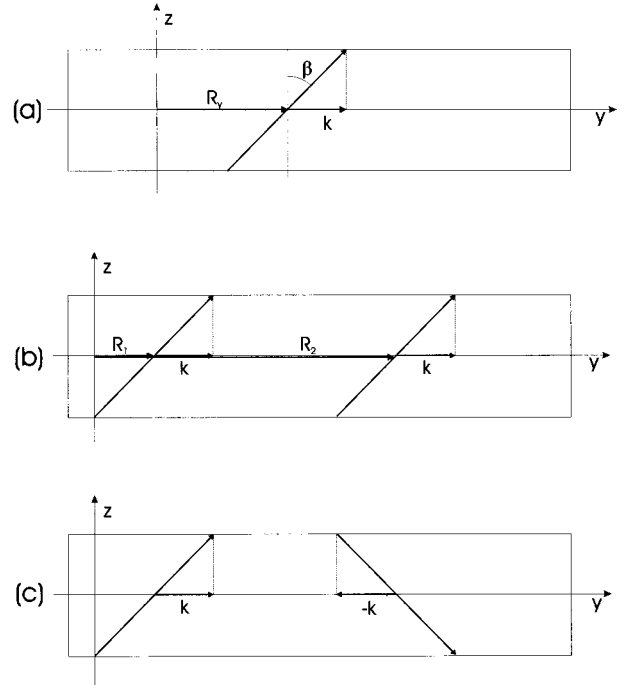


FIG. 2. (a) A tilted straight magnetic vortex crossing a film, (b) parallel tilted vortices, and (c) vortices symmetrical with respect to plane  $z=0$  (note that the sign of vector  $\mathbf{k}$  is not connected to the sign of the field).

$$\Phi_{\mathbf{q}}^z = \Phi_0 \exp(-i\mathbf{q} \cdot \mathbf{R} - i\mathbf{k} \cdot \mathbf{q}z) \quad (7)$$

and then Eqs. (1), (2), and (4) to

$$\left( Q^2 - \frac{\partial^2}{\partial z^2} \right) h_{\mathbf{q}}^j(z) = \lambda^{-2} \Phi_{\mathbf{q}}^j(z), \quad |z| \leq d,$$

$$\left( q^2 - \frac{\partial^2}{\partial z^2} \right) h_{\mathbf{q}}^j(z) = 0, \quad |z| \geq d, \quad (8)$$

with  $Q^2 = q^2 + \lambda^{-2}$ . Making use of the boundary conditions and Eq. (2) inside the sample one finds for the field components inside the superconductor

$$h_{\mathbf{q}}^z = A \frac{q \cos \mathbf{k} \cdot \mathbf{q}d/2 - \mathbf{k} \cdot \mathbf{q} \sin \mathbf{k} \cdot \mathbf{q}d/2}{Q \sinh Qd/2 + q \cosh Qd/2} \cosh Qz - iA \frac{q \sin \mathbf{k} \cdot \mathbf{q}d/2 + \mathbf{k} \cdot \mathbf{q} \cos \mathbf{k} \cdot \mathbf{q}d/2}{Q \cosh Qd/2 + q \sinh Qd/2} \sinh Qz - A e^{-i\mathbf{k} \cdot \mathbf{q}z},$$

$$h_{\mathbf{q}}^x = \frac{iq_x}{q} A \left[ \frac{Q \cos \mathbf{k} \cdot \mathbf{q}d/2 \sinh Qd/2 + \mathbf{k} \cdot \mathbf{q} \sin \mathbf{k} \cdot \mathbf{q}d/2 \cosh Qd/2}{Q \sinh Qd/2 + q \cosh Qd/2} \frac{\sinh Qz}{\sinh Qd/2} - i \frac{Q \sin \mathbf{k} \cdot \mathbf{q}d/2 \cosh Qd/2 - \mathbf{k} \cdot \mathbf{q} \cos \mathbf{k} \cdot \mathbf{q}d/2 \sinh Qd/2}{Q \cosh Qd/2 + q \sinh Qd/2} \frac{\cosh Qz}{\cosh Qd/2} \right],$$

$$h_{\mathbf{q}}^y = \frac{q_y}{q_x} h_{\mathbf{q}}^x + kA \left[ \frac{\cosh Qz}{\cosh Qd/2} \cos \mathbf{k} \cdot \mathbf{q}d/2 - i \frac{\sinh Qz}{\sinh Qd/2} \sin \mathbf{k} \cdot \mathbf{q}d/2 - e^{-i\mathbf{k} \cdot \mathbf{q}z} \right], \quad (9)$$

where  $A = -\Phi_0 e^{-i\mathbf{q}\cdot\mathbf{R}}/\lambda^2 [Q^2 + (\mathbf{k}\cdot\mathbf{q})^2]$ , and outside the superconductor

$$h_{\mathbf{q}}^i(z) = h_{\mathbf{q}}^i(\pm d/2) \exp\left[q\left(\frac{d}{2} - |z|\right)\right], \quad \pm z \geq d/2. \quad (10)$$

The expressions (9) and (10) are valid for a vortex located far from the edges of the film relative to the transverse penetration depth  $\Lambda$ ,  $W/2 - |x| \gg \Lambda$ , and may be used for any vortex orientation, not only tilted along the  $y$  axis. In general,  $h_{\mathbf{q}}^y$  and  $h_{\mathbf{q}}^x$  would mean the field components parallel and transverse to the vector  $\mathbf{k}$ , respectively. Since the condition  $d \ll \lambda$  was used so far for justifying the assumption of a straight vortex [Eq. (5)], the expressions (9) and (10) are valid for a superconducting plate of any thickness. Particularly, in the case  $\mathbf{k}=0$  one finds from Eq. (9) a field of the vortex normal to the plate of finite thickness,<sup>25</sup> and then, in the limit  $d \ll \lambda$ , the well-known Pearl solution for the vortex in a thin film.<sup>22</sup>

Let us note that for the evaluation of the tilted vortex characteristics one cannot use the above Pearl approximation, where the film is considered as having a zero thickness. In the latter case, a current may flow only in the  $xy$  plane, contributing, thus, only to the magnetic moment perpendicular to the film. For this Pearl vortex, the only essential characteristic length in space is  $\Lambda$ . In the tilted vortex case, the finite  $k$  means the appearance of a nonzero magnetic moment component parallel to the film and a nonzero current density component  $j_z$  normal to the surface whatever thin the film is. This leads to the space dependence of all the quantities on the scale of the film thickness  $d$ . We proceed now with a calculation of the free energy of the tilted vortex and a pair of interacting tilted vortices.

### C. Free energy of straight tilted vortices in a superconducting plate of arbitrary thickness

The conventional expression for the free energy,<sup>26</sup>

$$F = \frac{1}{8\pi} \int_{|z| \leq d/2} [\mathbf{h}^2 + \lambda^2 (\text{curl } \mathbf{h})^2] dV + \frac{1}{8\pi} \int_{|z| \geq d/2} \mathbf{h}^2 dV, \quad (11)$$

may be easily expressed in terms of the Fourier components by using Eqs. (8):

$$F = \frac{1}{8\pi} \int_{|z| \leq d/2} dz \int \frac{d^2\mathbf{q}}{(2\pi)^2} \mathbf{h}_{-\mathbf{q}} \Phi_{\mathbf{q}} + \frac{\lambda^2}{8\pi} \int \frac{d^2\mathbf{q}}{(2\pi)^2} \times \left[ h_{-\mathbf{q}}^x \frac{\partial h_{\mathbf{q}}^x}{\partial z} + h_{-\mathbf{q}}^y \frac{\partial h_{\mathbf{q}}^y}{\partial z} - h_{-\mathbf{q}}^z \frac{\partial h_{\mathbf{q}}^z}{\partial z} \right] \Big|_{z=-d/2}^{z=d/2}. \quad (12)$$

The second (surface) term in Eq. (12) vanishes if the vortex does not cross the plate surface even if the field itself does not vanish at the surface, as was shown in Ref. 17. Thanks to a linearity of the London approximation, the above expression is valid for any number of vortices. In the last case, the superposition of the source functions [Eq. (2)] should be taken for  $\Phi$  and the superposition of the solutions to Eqs. (9) and (10) corresponding to different vortices should be taken for  $\mathbf{h}$  in Eq. (12).

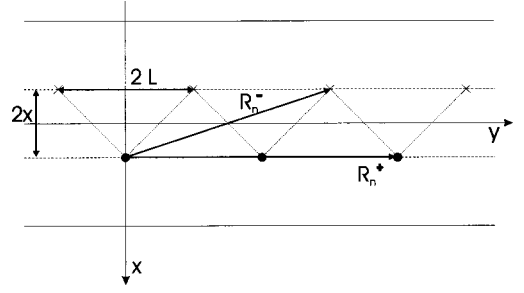


FIG. 3. The location of the upward- ( $\mathbf{R}_n^+$ ) and downward- ( $\mathbf{R}_n^-$ ) directed vortices in a vortex chain.

We consider first the interaction energy of two equally tilted vortices  $U_+(\mathbf{R})$ . Then, one should use for  $\mathbf{h}$  in Eq. (12) the field  $\mathbf{h} = \mathbf{h}^1 + \mathbf{h}^2$  generated by the two vortices located in positions  $\mathbf{R}_1$  and  $\mathbf{R}_2$  [see Fig. 2(b)]. The only difference in the field expressions (9) and (10) for vortices 1 and 2 is, in this case, determined by the position vectors  $\mathbf{R}_{1,2}$  of the multiplier  $A$ . For our purpose we also need to calculate the interaction energy  $U_-(\mathbf{R})$  of vortices symmetrical with respect to the plane  $z=0$ . They have opposite signs of the  $z$  component of the field and are equally tilted with respect to the positive  $y$  direction as is shown in Figs. 1(b) and 2(c). To calculate the interaction energy in this case one should take  $\mathbf{h} = \mathbf{h}_1 + \mathbf{h}_2$  and use for one of the vortices the expressions (9) with the changed signs of both  $\mathbf{k}$  and  $A$ .

Upon the substitution of the field expressions (9) in Eq. (12) one finds

$$U_{\pm}(\mathbf{R}) = \frac{\varepsilon_0 d}{2\pi} \int d^2\mathbf{q} u_{\pm}(\mathbf{q}) \cos \mathbf{q} \cdot \mathbf{R}, \quad \mathbf{R} = \mathbf{R}_1 - \mathbf{R}_2, \quad (13)$$

where  $\varepsilon_0 = (\Phi_0/4\pi\lambda)^2$ . Exact expressions for the functions  $u_{\pm}(\mathbf{q})$  are calculated in the Appendix and are rather cumbersome. In the following, we will use approximate expressions taking into account the inequality  $d \ll \lambda$ . The self-energy of the tilted vortex may be found from Eq. (13) by taking  $\mathbf{R} = 0$ . It differs from the known expression<sup>19</sup> by a nonessential coefficient of the order of unity. Now we are in a position to consider the vortex chain energy.

### D. Gibbs free energy of the vortex chain and spiral instability of a single FL parallel to the current

Let us consider a thin superconducting film described above in Sec. II B. An external magnetic field of magnitude  $H$  slightly above  $H_{c1}(d)$  is applied in the positive  $y$  direction and a transport current  $I$  flows the same direction. Flux lines of the external field are supposed to be located far enough away from each other to neglect the interaction. At sufficiently high currents the straight FL's become unstable. As a result of the left-handed spiral development of the FL initially lying along the  $y$  axis ( $x=z=0$ ) two chains of vortices are formed as described in Sec. II A (see Fig. 1): upward-directed vortices are located at the positions  $(x, 2nL)$  and downward-directed ones are at the positions  $(-x, (2n-1)L)$ , where  $n$  is integer, and  $2L$  and  $2x$  are the pitch length and width of the spiral-like chain configuration, respectively (Fig. 3). All the vortices are inclined by the same angle with regard to the positive direction of the  $y$  axis.

Energetically, all the vortex positions are equivalent. This enables us to calculate the energy of the chain per unit length along the  $y$  axis as the energy of one of the vortices divided by  $L$  as follows:

$$F = \frac{1}{L} \sum_n [U_+(\mathbf{R}_n^+) + U_-(\mathbf{R}_n^-)], \quad (14)$$

where  $\mathbf{R}_n^+ = (0, 2nL)$  and  $\mathbf{R}_n^- = (-2x, (2n-1)L)$  denote the distances between the test vortex located at  $(x, 0)$  and vortices of the same and opposite vorticity, respectively (see Fig. 3). The summation extends over all integer  $n$  including  $n=0$ , accounting for the test vortex self-energy  $U_+(\mathbf{R}_0^+ = 0)$ .

The space dependence enters the energy expressions  $U_\pm(\mathbf{R})$  only through the circular functions [Eq. (13)]: therefore the evaluation of the energy Eq. (14) may be simplified by using the relations

$$\begin{aligned} \sum_n \cos \mathbf{q} \cdot \mathbf{R}_n^+ &= \sum_n \cos(q_y 2nL) = \frac{\pi}{L} \sum_n \delta\left(q_y - \frac{\pi}{L} n\right), \\ \sum_n \cos \mathbf{q} \cdot \mathbf{R}_n^- &= \sum_n \cos[q_y(2n-1)L - 2xq_x] \\ &\rightarrow \frac{\pi}{L} \cos(2xq_x) \sum_n (-1)^n \delta\left(q_y - \frac{\pi}{L} n\right), \end{aligned} \quad (15)$$

where  $n$  is an integer. In the derivation of the last formula the evenness of the integrand in Eqs. (13) and (15) was used.

Let us assume that short pitch lengths  $L$  are typical for instability process and  $\xi \ll L < \pi d$ . Then  $|q_y| = \pi|n|/L > d^{-1}$  for any  $n \neq 1$ . Taking this into account one finds for functions  $u_\pm(\mathbf{q})$  the following approximations (see the Appendix):

$$\begin{aligned} u_+(\mathbf{q}) &= \frac{1+k^2}{Q^2 + (\mathbf{k} \cdot \mathbf{q})^2} + \frac{\theta(1-qd)}{Q^2 + (\mathbf{k} \cdot \mathbf{q})^2} \left( \frac{1 + \lambda^2(\mathbf{k} \cdot \mathbf{q})^2}{\lambda^2(q + 1/2\Lambda)^2} - k^2 \right), \\ u_-(\mathbf{q}) &= -\frac{1-k^2}{Q^2 + (\mathbf{k} \cdot \mathbf{q})^2} \frac{\sin \mathbf{k} \cdot \mathbf{q} d}{\mathbf{k} \cdot \mathbf{q} d} \\ &\quad - \frac{\theta(1-qd)}{Q^2 + (\mathbf{k} \cdot \mathbf{q})^2} \left( \frac{1 + \lambda^2(\mathbf{k} \cdot \mathbf{q})^2}{\lambda^2(q + 1/2\Lambda)^2} + k^2 \right), \end{aligned} \quad (16)$$

where  $\theta(x)$  is the Heaviside step function.

For simplicity the development of the chain is considered in the region  $x \leq d/2$ , which allows one to find an analytic expression for the free energy:

$$\begin{aligned} F &= \frac{\varepsilon_0 d \sqrt{1+k^2}}{L} \left[ \gamma + \ln\left(\frac{L}{\pi\xi}\right) \right] + \frac{\varepsilon_0 d}{L^2} \left[ 2k^2 d + \pi x(1-k^2) \right. \\ &\quad \left. + x^2 \left( \frac{2\pi k^2}{\lambda} - 2k^2/d - \frac{1+2\ln 2\lambda/d}{\Lambda} \right) \right]. \end{aligned} \quad (17)$$

In the above evaluation, the logarithmically divergent series  $\sum_n^{-1}$  was cut off at the number  $N \sim L/\pi\xi$ , which corre-

sponds to the usual momentum cutoff  $q_y \approx 1/\xi$  in the evaluation of the vortex self-energy in the London approximation.<sup>26</sup>

The instability first nucleates, presumably, as a smooth left-handed helical distortion of the linear FL and then breaks into a vortex chain. The pitch length of this structure is determined at the earlier stage of nucleation since after the vortex chain formation the vortices move perpendicular to the current. In our model, we treat the FL instability in a single description as if the vortex chains were formed from the very beginning of the process at  $x=0$ . The optimum parameters of the first unstable mode and the critical current of this will be determined in a self-consistent manner and then compared with the known conditions of the helical instability. We keep in mind that the critical current found in such a manner may be underestimated because of the shortened total length of FL's but may also be overestimated thanks to the large energy of the strongly nonuniform chain structure. For example, the initial energy of the vortex-antivortex chain at  $x=0$ ,  $k=0$  following from Eq. (17), i.e.,

$$F = \frac{\varepsilon_0 d}{L} \left[ \gamma + \ln\left(\frac{L}{\pi\xi}\right) \right], \quad (18)$$

is larger than the initial FL's energy per unit length  $F_0 = \varepsilon_0 \ln(d/2\xi)$  (Ref. 14) at the lowest reasonable pitch length  $L = \pi\xi$  but is smaller than  $F_0$  at  $L = \pi d$ .

The Gibbs free energy of the spiral-like chain structure [Figs. 1(b), 1(c), and 3] (Ref. 27),

$$G(I, H) = F - \Delta W_H - \Delta W_I, \quad (19)$$

including the contribution of the external field,  $\Delta W_H$ , and the work done by the source of the transport current,  $\Delta W_I$ , may be negative. The instability sets in when  $G$  is not only negative but also less than a Gibbs free energy of the initial linear FL,  $G_0(H)$ , which is also negative at  $H > H_{c1}(d)$ . It is clear that it should happen at some value of the current since  $G_0(H)$  is current independent.

The magnetic field contribution may be directly calculated using Eqs. (9) as

$$\begin{aligned} \Delta W_H &= \frac{1}{4\pi L} \int \mathbf{H} \mathbf{h} dV = \frac{kH\Phi_0 d}{4\pi L} \left( 1 - \frac{\tanh d/2\lambda}{d/2\lambda} \right) \Big|_{d \ll \lambda} \\ &\rightarrow \frac{\varepsilon_0 d}{L} \frac{2}{3} kh \ln \frac{d}{\xi}, \end{aligned} \quad (20)$$

where the dimensionless field  $h = H/H_{c1}(d)$ ,  $H_{c1}(d) = (2\Phi_0/\pi d^2) \ln d/\xi$ .<sup>14</sup>

To calculate the transport current contribution  $\Delta W_I$  we suppose the Meissner distribution of the current in the film:<sup>27,28</sup>

$$j(x) = \frac{I}{\pi d \sqrt{(W/2)^2 - x^2}}. \quad (21)$$

Then the work done by the source of the transport current as the vortex moves from a film center through a distance  $x$  in a positive  $x$  axis direction is

$$\int_0^x \frac{j(x)\Phi_0 d}{c} dx = \frac{I\Phi_0}{\pi c} \arcsin \frac{2x}{W}. \quad (22)$$

Let us note that this value is independent of the vortex tilt angle, since the  $z$  projection of the vortex length perpendicular to current remains constant and equal to  $d$ . Finally, one gets

$$\Delta W_I = \frac{\varepsilon_0 d}{L} h_i \ln \left( \frac{\lambda}{\xi} \right) \frac{\arcsin(2x/W)}{d/W} \approx \frac{\varepsilon_0 d}{L} h_i \ln \left( \frac{\lambda}{\xi} \right) \frac{2x}{d}, \quad (23)$$

for  $x \ll W$ . Here the dimensionless current self-field is introduced as  $h_i = H_I/H_{c1}$  where  $H_I = 4I/Wc$  is the magnitude of the current self-field over the film center.

The vortex chain is supposed to nucleate initially at  $x \approx d/2$  [Fig. 1(a)] and then expand, driven by the Lorentz force exerted upon the vortices by the transport current. We take for the criterium of the vortex chain nucleation the condition

$$\Delta G(k, L) = G(I, H)|_{x=d/2} - G_0(H) \leq 0, \quad (24)$$

where

$$G_0(H) = \varepsilon_0 (1-h) \ln \frac{d}{2\xi} \quad (25)$$

is the Gibbs energy of the initial linear FL lying parallel to external field inside the film.<sup>14</sup>

The numerical study of the function  $\Delta G(k, L)$  shows a deep minimum of energy located at some values  $k < 1$  and  $L \approx d$  in the field range  $1 < h < 4$ ,  $h_i \sim 1$  (see Fig. 4). This is in qualitative agreement with the results for the single FL helical instability in thin films,<sup>17</sup>  $L_c \sim d/h_i$ ,  $h_i \sim \sqrt{h-1} < 1$ , and thin wires,<sup>32</sup>  $L_c \sim d/\sqrt{h-1}$ ,  $h \gg 1$ . We need now to estimate the critical current of the chain instability and to compare it to that of a helical instability in thin films.<sup>17</sup>

### E. Critical current of the chain instability of a single flux line

In this section we first simplify the expression (19) for the energy of the chain structure by taking into account the actual parameter region. Then we find values for the vortex tilt  $k_0$  and pitch length  $L_0$ , delivering a minimum of  $G(I, H)$ . The chain with these parameters  $k_0$  and  $L_0$  is the first to nucleate when the condition  $\Delta G(k, L) = 0$  is first satisfied at some critical value of the transport current.

The Gibbs free energy (19) with account of  $L \sim d$ ,  $k < 1$ ,  $2x = d$  is reduced to

$$\begin{aligned} G(k, L) = & \frac{\varepsilon_0 d \sqrt{1+k^2}}{L} \left[ \gamma + \ln \left( \frac{L}{\pi \xi} \right) \right] \\ & + \frac{\varepsilon_0 d^2}{L^2} \left[ \pi + k^2 \left( 3 - \pi + \frac{\pi d}{\lambda} \right) \right] \\ & - \frac{2\varepsilon_0 d k h}{3L} \ln \frac{d}{2\xi} - \frac{\varepsilon_0 d h_i}{L} \ln \frac{\lambda}{\xi}, \end{aligned} \quad (26)$$

where  $\gamma = 0.5772 \dots$  is the Euler constant.

The equations for the values  $k_0$  and  $L_0$  are given by the conditions  $\partial G/\partial k = 0$  and  $\partial G/\partial L = 0$  and solved numeri-

cally. Thereafter, the resulting  $k_0$  and  $L_0$  depending on the field and current should be substituted in Eq. (24) to determine the critical value of  $h_i$  corresponding to the critical current of the chain instability. An analytical solution of the above transcendental equations is impossible. For the following numerical study we need to define the parameters involved. Let us consider a  $\text{YBa}_2\text{Cu}_3\text{O}$  thin film at temperature  $T = 77$  K having a penetration depth  $\lambda = 220$  nm and  $\xi = 3.6$  nm.<sup>29</sup> Let the thickness  $d$  be of  $100 \text{ nm} < \lambda$  and the width  $W$  be of  $50 \mu\text{m}$ .

The results of the numerical solution are presented in Fig. 5. At low fields the 2D vortices are far from each other and their interaction with the external field dominates over the mutual interaction. The linear growth of the tilt angle at low fields reproduces the behavior known for the isolated vortex crossing a film<sup>19</sup> as well as for the tilted FLL (Refs. 18–21) and is quite understandable. As an evaluation of  $k$  in this region, one can take  $L = \lambda$  and find by the variation of Eq. (26)

$$k \approx \frac{2h \ln(1/2\xi)}{3[\gamma + \ln(\lambda/\pi\xi)]}. \quad (27)$$

This linear dependence is shown in Fig. 5 (dashed line) and describes well the low-field behavior of  $k$ . With growing field, the tilt angle grows while the intervortex distance decreases. When the equality  $k = L/d$  is reached and a saw-toothed structure is formed [Fig. 1(b)] the intervortex interaction becomes large enough to change the behavior of the tilt angle. Further growth of  $k$  is impossible since vortex structures with  $k > L/d$  are meaningless. Then, in the high-field region, the minimum of energy is achieved at the line  $k = L/d$  as is shown in Fig. 6.

The pitch length  $L$  decreases monotonously in the whole field region and agrees satisfactorily with the above cited results for the helical instability. It is reasonable since the saw-toothed structure of the instable mode [dashed line in Fig. 1(b)] formed already in fields  $h > 1.6$  may be treated as a discrete analog of the helical mode. Let us note that  $L$  remains less than  $\pi d$  even at the lowest considered field value of  $H = 1.002 H_{c1}(d)$ , which supports the initial assumption in Sec. II D.

The reduced self-field  $h_{in}$  proportional to the current of instability  $j_{in}$  may be well fitted in the region  $1.5 < h < 3$  by the linear dependence

$$h_{in,chain} = 1.06 + 0.15(h-1). \quad (28)$$

For the thin film considered above, the self-field of the critical current of the helical instability taken from Ref. 17 is close to the above result in the same field region:

$$h_{in,helix} = \frac{d}{2\lambda} \sqrt{\frac{H_{c1}(d)}{2H_{c1}}} \sqrt{h-1} = 0.80 \sqrt{h-1}. \quad (29)$$

We should make clear that it does not make much sense to consider a single flux-line instability in fields well above the  $H_{c1}(d)$  where a FLL is formed and one cannot neglect intervortex interaction. Nevertheless, it is clear from the above consideration that short-wave instable modes are favored in thin films and they may be described in the vortex chain model.

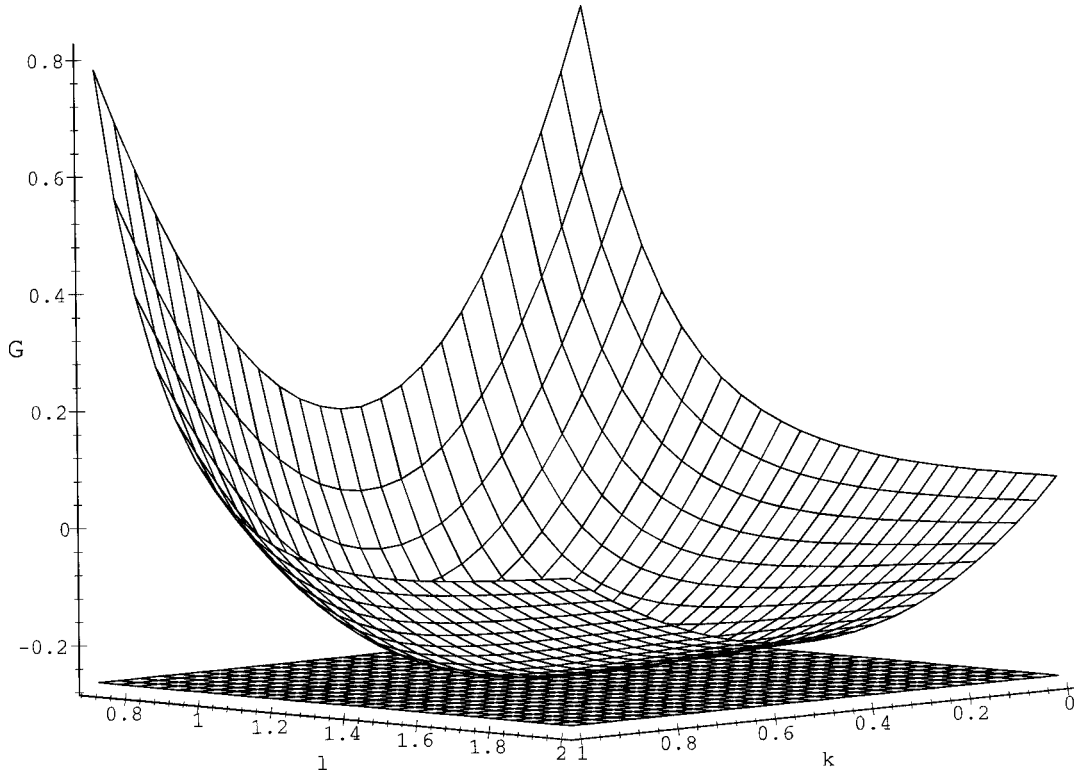


FIG. 4. The relief of the Gibbs free energy of the vortex chain  $G$  over the plane  $(k, l)$ , where  $k$  is the tangent of the vortex tilt angle with respect to the normal to the film and  $l = L/d$  is the vortex structure pitch length in units of the film thickness  $d$ . In the minimum, the energy surface first touches the plane which presents the energy of the initial FL.

### III. CHAIN INSTABILITY OF A ONE-DIMENSIONAL FLUX-LINE LATTICE IN A THIN FILM

#### A. Qualitative picture of the instability of a one-dimensional FLL

In this section we consider a more realistic case of a flux-line lattice parallel to a thin film surface. The one-dimensional FLL (one row of vortices) first enters the film as the external field first attains the value of  $H_{c1}(d)$ .<sup>14</sup> The energy of the FLL per unit volume is<sup>14</sup>

$$G_0(h, a) = \frac{\varepsilon_0}{ad} \left[ 1 - h + \frac{2}{\ln(d/\xi)} \times \ln \left( \frac{1 + \exp(-\pi a/d)}{1 - \exp(-\pi a/d)} \right) \ln(d/2\xi) \right], \quad (30)$$

where  $a$  is the intervortex distance. By minimizing  $G_0(h, a)$  with respect to  $a$  one can find the latter as a function of the field,  $a(h)$  (see Fig. 7), which is important for the following.

As follows from commensurability, at fields  $H = H_n = (\sqrt{3}\Phi_0/2d^2)n^2$  an  $n$ -row FLL is formed in thin films.<sup>30</sup> The two-row FLL formation at  $H_2 \approx 2H_{c1}(d)$  does not affect much the creation of an instability. But at higher fields  $H \approx H_3$ , a three-row FLL is formed and the instability can no longer be treated in simple two-dimensional terms. In recent precise simulations,<sup>31</sup> Carneiro found values of  $H_2 \approx 2.2H_{c1}(d)$  and  $H_3 \approx 4.3H_{c1}(d)$ . For further consideration we restrict ourselves to the field region  $H < 3H_{c1}(d)$ .

As is easily seen from Fig. 7, the intervortex distance within the first row of vortices even slightly above the  $H_{c1}(d)$  is of the order of  $d < \lambda$ . That means that, in fact, one cannot neglect the interaction of FL's at any field.

We apply now the vortex chain model to the problem of the one-dimensional FLL instability. The latter may be realized as follows. If the neighboring spiral-like chain structures are shifted against each other by a half period along the  $y$  axis, as is shown in Fig. 8, the vortices of opposite vorticity become nearest neighbors. Then the attraction between them favors the instable spiral expansion. When the attracting vortices meet, they cannot completely annihilate since both are tilted in the positive  $y$  direction. Thus, as a result of

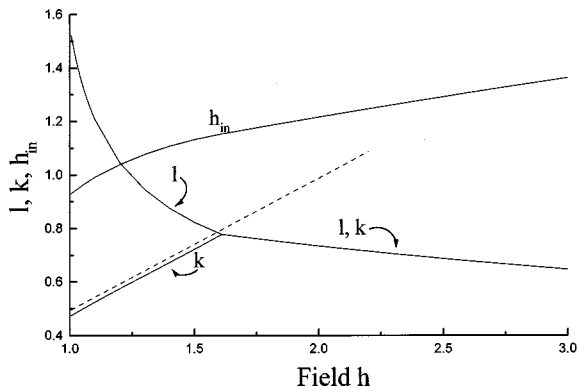


FIG. 5. Critical parameters of the chain instability of a single flux line.  $h_{in}$  is the dimensionless self-field of the critical current of instability,  $l = L/d$  is the pitch length of the most unstable mode, and  $k = \tan \beta$ , where  $\beta$  is the tilt angle of vortices in the vortex chain. The straight (dashed) line presents the field dependence of the tilt angle of an isolated tilted 2D vortex and approximates well the low-field behavior of  $k$ .

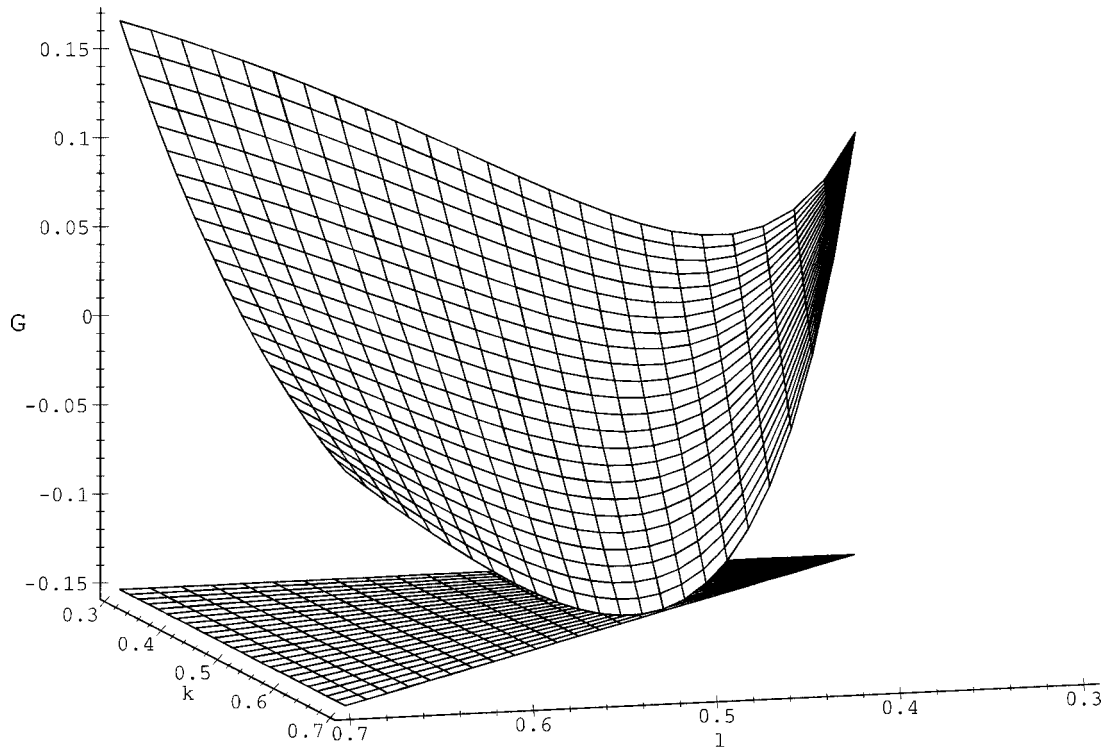


FIG. 6. The Gibbs free energy  $G$  of the vortex chain structure resulting from the instability of a one-dimensional FLL. The relief of  $G$  is shown over the plane  $(k, l)$  with regard to the physical restriction  $k \leq l = L/d$ , where  $k$  is the tangent of the vortex tilt angle with respect to the normal to the film and  $l = L/d$  is the vortex structure pitch length in units of the film thickness  $d$ . The conditional minimum is seen to be reached at the boundary line  $k = l$  where the energy first attains the plane which presents the energy of the initial FLL.

$z$ -component annihilation, the reconnection of vortices and formation of straight FL's parallel to the film happen, which lie in the middle between the former FL positions. Due to the exit of the upward-directed chain of vortices through the  $x = W/2$  edge of the film and downward-directed chain of vortices through the  $x = -W/2$  edge of the film (see Fig. 8), the number of FL's in the sample becomes less by 1. This state is unstable against the entry of one more FL to restore the initial thermodynamic equilibrium state. After recovering the initial state the instability may repeat. We shall call this scenario the antiphase mode of instability.

As is known from earlier works,<sup>10,11</sup> the lowest current of instability in bulk superconductors is achieved at a uniform helical distortion of the FLL. In terms of vortex chains, this means that every FL is deformed the same way as is shown in Fig. 9. We shall call this scenario the uniform mode of instability. Let us determine now the critical currents triggering the above modes of instability of the one-dimensional FLL.

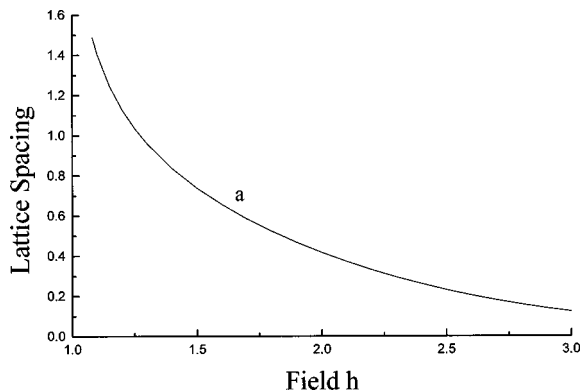


FIG. 7. Intervortex distance (lattice spacing)  $a$  in units of a film thickness,  $d$ , within a one-dimensional flux-line lattice parallel to a thin film surface and to the external magnetic field vs the applied field  $h = H/H_{c1}(d)$ .

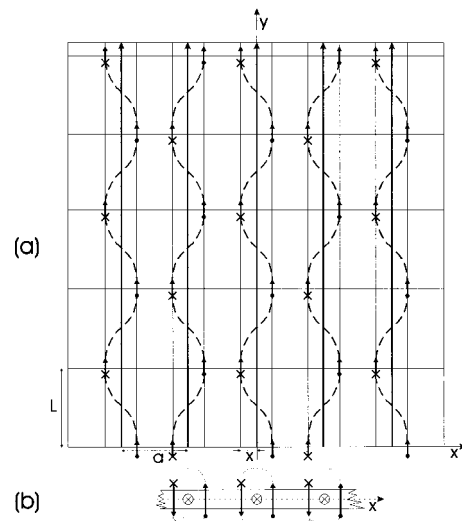


FIG. 8. Schematic projections of the chain instability of a one-dimensional flux-line lattice on the  $xy$  (a) and  $xz$  (b) planes for the antiphase mode. The downward-directed 2D vortices are marked with a cross.



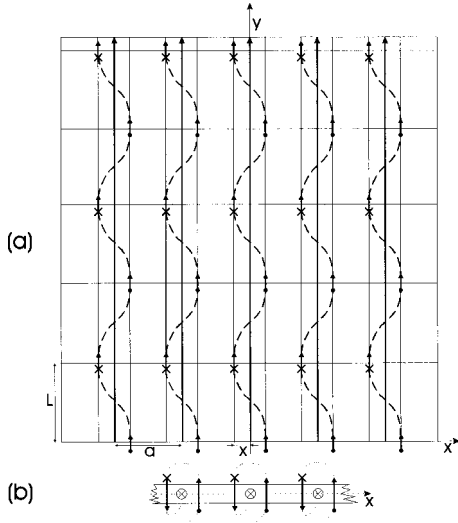


FIG. 9. Schematic projections of the chain instability of a one-dimensional flux-line lattice on the  $xy$  (a) and  $xz$  (b) planes for the uniform mode. The downward-directed 2D vortices are marked with a cross.

### B. Critical current of a spiral-like chain distortion of a one-dimensional FLL

Let the one-dimensional FLL be transformed into chains of tilted 2D vortices as is shown in Fig. 8 (antiphase mode). The upward- and downward-directed vortices both occupy two sorts of positions, respectively,

$$\begin{aligned} \mathbf{R}_1^+ &= (2ma + x, 2nL), & \mathbf{R}_2^+ &= ((2m-1)a + x, (2n-1)L), \\ \mathbf{R}_1^- &= (2ma - x, (2n-1)L), & \mathbf{R}_2^- &= ((2m-1)a - x, 2nL), \end{aligned} \quad (31)$$

where  $m$  and  $n$  are integers.

All the vortices are in equivalent positions and have the same energy. Since the transverse distance between the chains is defined by the initial field-dependent spacing  $a$  ( $h$ ) and the longitudinal spacing is the pitch length  $L$  (Fig. 8), the energy of the system per unit volume,  $F$ , equals the energy per one vortex divided by  $aLd$ . Let us choose the vortex located at  $\mathbf{R}_1^+ = (x, 0)$  as a test vortex. Then the distances from this vortex to the other upward- and downward-directed ones are, respectively,

$$\Delta\mathbf{R}_1^+(m, n) = (2ma, 2nL),$$

$$\Delta\mathbf{R}_2^+(m, n) = ((2m-1)a, (2n-1)L),$$

$$\Delta\mathbf{R}_1^-(m, n) = (2ma - 2x, (2n-1)L),$$

$$\Delta\mathbf{R}_2^-(m, n) = ((2m-1)a - 2x, 2nL). \quad (32)$$

Now, the energy  $F$  reads as

$$\begin{aligned} F &= \frac{1}{aLd} \sum_{m,n} [U_+(\Delta\mathbf{R}_1^+(m, n)) + U_+(\Delta\mathbf{R}_2^+(m, n)) \\ &\quad + U_-(\Delta\mathbf{R}_1^-(m, n)) + U_-(\Delta\mathbf{R}_2^-(m, n))]. \end{aligned} \quad (33)$$

Making use of the relations (15) one can transform Eq. (33) into:

$$\begin{aligned} F &= \frac{\pi\varepsilon_0}{2a^2L^2} \sum_{m,n} \left[ u_+(\mathbf{q}_{m,n}) [(-1)^{m+n} + 1] \right. \\ &\quad \left. + u_-(\mathbf{q}_{m,n}) [(-1)^m + (-1)^n] \cos\left(\frac{2\pi x}{a}m\right) \right], \end{aligned} \quad (34)$$

where  $\mathbf{q}_{m,n} = [(\pi/a)m, (\pi/L)n]$ .

The picture shown in Fig. 8 makes sense for  $k < L/d$  and  $0 < x < a/2$ . Since the initial vortex spacing  $a < \pi d$  at all fields, but one very close to  $H_{c1}(d)$ , and  $L$  is supposed to be less than  $\pi d$  too, the  $q_{m,n} > d^{-1} > \lambda^{-1}$  for any  $m \neq 0$  or  $n \neq 0$ . That allows one to use for the functions  $u_{\pm}(\mathbf{q})$  the following approximations (see the Appendix):

$$\begin{aligned} u_+(\mathbf{q}) &= \frac{1+k^2}{Q^2 + (\mathbf{k} \cdot \mathbf{q})^2} + 2 \frac{(\mathbf{k} \cdot \mathbf{q})^2 - k^2 q^2}{qd[Q^2 + (\mathbf{k} \cdot \mathbf{q})^2]^2}, \\ u_-(\mathbf{q}) &= -\frac{1-k^2}{Q^2 + (\mathbf{k} \cdot \mathbf{q})^2} \frac{\sin(\mathbf{k} \cdot \mathbf{q}d)}{(\mathbf{k} \cdot \mathbf{q})d} - \frac{2}{d[Q^2 + (\mathbf{k} \cdot \mathbf{q})^2]^2} \\ &\quad \times \left[ \frac{[(\mathbf{k} \cdot \mathbf{q})^2 - k^2 q^2] \cos(\mathbf{k} \cdot \mathbf{q}d)}{q} \right. \\ &\quad \left. + (\mathbf{k} \cdot \mathbf{q})(1+k^2) \sin(\mathbf{k} \cdot \mathbf{q}d) \right], \end{aligned} \quad (35)$$

if  $m \neq 0$  or  $n \neq 0$ . For the case  $m = n = 0$  one finds  $u_{\pm}(\mathbf{q}_{0,0}) = \pm 4\Lambda^2$ .

Substituting Eqs. (35) into Eq. (34) and performing the summation over  $m$  one finds

$$\begin{aligned} F &= \frac{\varepsilon_0 \pi}{L^2} \left[ \frac{1}{6} k^2 + (1-k^2) \frac{x}{a} \left( 1 - \frac{2x}{a} \right) \right] + \frac{\varepsilon_0}{aL} \sqrt{1+k^2} \sum_{n=1}^{\infty} \frac{\cosh[(\pi an/L) \sqrt{1+k^2}] + (-1)^n}{n \sinh[(\pi an/L) \sqrt{1+k^2}]} \\ &\quad - \frac{\varepsilon_0(1-k^2)}{\pi k a d \sqrt{1+k^2}} \sum_{n=1}^{\infty} \frac{1}{n^2} \sin\left(\frac{k\pi dn}{L}\right) \frac{\left[ \cosh[(2\pi xn/L) \sqrt{1+k^2}] + (-1)^n \cosh\left(\frac{\pi an(1-2x/a)}{L} \sqrt{1+k^2}\right) \right]}{\sinh[(\pi an/L) \sqrt{1+k^2}]} \\ &\quad - \frac{\pi k^2}{6a^2(1+k^2)} \left( 1 - \frac{kd}{L} \right) \left( 1 - 2 \frac{kd}{L} \right) - \frac{k^2 a}{2\pi^2 L^2 d} \left( 1 + \cos \frac{4\pi x}{a} \right). \end{aligned} \quad (36)$$

To account for the work done by the external sources of field and transport current one should add to Eq. (36) the expressions (20) and (23) normalized per unit volume and obtain

$$G = F - \frac{\varepsilon_0}{aL} \frac{2}{3} kh \ln\left(\frac{d}{2\xi}\right) - h_i \frac{\varepsilon_0}{dL} \ln\left(\frac{\lambda}{\xi}\right) \frac{2x}{a}. \quad (37)$$

In the above formula,  $h_i = H_i/H_{c1}$ , where  $H_i = 2\pi jd/c$  is a local current self-field over the film and  $j$  is a local current density. In what follows, we suppose that, in a resistive state, the current is distributed approximately uniformly over the film cross section.

The above Gibbs energy of the system should be compared with the Gibbs energy of the initial linear FLL (30). The critical current of instability is achieved when the difference  $G_{min} - G_0(h, a)$  first becomes negative.  $G$  is a complicated function of three variables  $k$ ,  $L$ , and  $x$  and possesses a rather nontrivial 3D relief. The summation in Eq. (36) cannot be performed analytically. On the other hand, the truncation of the sums produces unphysical minima, complicating the numerical analysis. To avoid these problems and, simultaneously, to account for the barrier nature of the instability nucleation we consider in what follows the energy  $g$  averaged over the distance which vortices pass in the course of the chain expansion:

$$g(k, l) = \frac{2}{a} \int_0^{a/2} dx G(k, L, x). \quad (38)$$

After this procedure the Gibbs energy reduces to

$$\begin{aligned} g = & \frac{\varepsilon_0 \sqrt{1+k^2}}{aL} \sum_{n=1}^{\infty} \frac{1}{n} \left\{ \coth\left(\frac{\pi an}{L} \sqrt{1+k^2}\right) + (-1)^n \right. \\ & \times \left[ \sinh\left(\frac{\pi an}{L} \sqrt{1+k^2}\right) \right]^{-1} \left. + \frac{\varepsilon_0}{L^2} \left[ \frac{\pi(1+k^2)}{12} - \frac{k^2 a}{2\pi^2 d} \right] \right. \\ & - \frac{\varepsilon_0 \pi}{12a^2} \left(1 - \frac{kd}{L}\right) \left(1 - \frac{2kd}{L}\right) - \frac{2\varepsilon_0 kh}{3aL} \ln \frac{d}{2\xi} \\ & \left. - \frac{\varepsilon_0 h_i}{2Ld} \ln \frac{\lambda}{\xi} \right\}. \quad (39) \end{aligned}$$

Let us take for granted that the instability occurs at a short wavelength  $L < \pi a$ , which will be justified later. Then, the hyperbolic functions in Eq. (39) may be approximated with good accuracy by exponents, which allows one to perform the summation analytically and to find finally

$$\begin{aligned} g = & \frac{\varepsilon_0 \sqrt{1+k^2}}{aL} \left\{ \gamma + \ln \frac{L}{\xi} - 2 \ln \left[ 1 + \exp\left(-\frac{\pi a}{L} \sqrt{1+k^2}\right) \right] \right\} \\ & + \frac{\varepsilon_0}{L^2} \left[ \frac{\pi(1+k^2)}{12} - \frac{k^2 a}{2\pi^2 d} \right] - \frac{\pi \varepsilon_0}{12a^2} \left(1 - \frac{kd}{L}\right) \left(1 - \frac{2kd}{L}\right) \\ & - \frac{2\varepsilon_0 kh}{3aL} \ln \frac{d}{2\xi} - \frac{\varepsilon_0 h_i}{2Ld} \ln \frac{\lambda}{\xi}. \quad (40) \end{aligned}$$

The instability onset is expected when the least possible magnitude of  $g$  first attains the magnitude of the Gibbs free energy of the initial FLL,  $G_0(h, a)$  [Eq. (30)]. The minimum

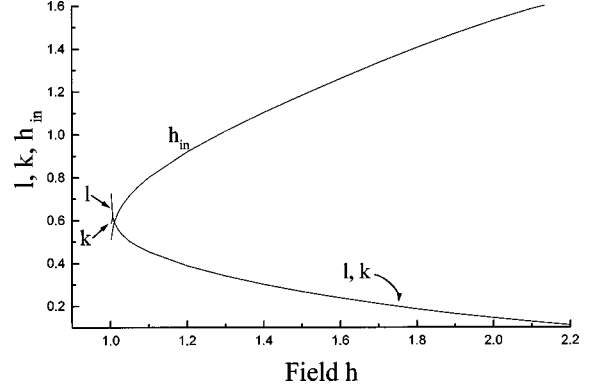


FIG. 10. Critical parameters of the chain instability of an one-dimensional flux-line lattice.  $h_{in}$  is a dimensionless self-field of the critical current of instability,  $l = L/d$  is the pitch length of the most unstable mode, and  $k = \tan \beta$  where  $\beta$  is the tilt angle of vortices in vortex chain.  $k$  grows in a narrow low-field region close to  $h = 1$ , then merges with  $l$ .

of  $g$  is achieved at some optimum values of pitch length  $L_0$  and tilt  $k_0$  defined by the equations

$$\frac{\partial g}{\partial k} = 0, \quad \frac{\partial g}{\partial L} = 0, \quad (41)$$

with account for the restriction  $k \leq L/d$ . Then the value of instability current  $j_{in}$  at a given magnetic field is obtained from the equation

$$g(k_0, L_0) = G_0(h, a). \quad (42)$$

A numerical analysis of Eqs. (41) and (42) shows that solutions  $k_0 \leq L_0$  exist only at very low fields  $1 < h < 1.006$  (Fig. 10). At higher fields, the absolute minimum of  $g$  shifts to the unphysical region  $k > L/d$ , and the physical minimum is achieved at  $k = L/d$  as well as is shown in Fig. 6. The last condition corresponds to the short-wave saw-toothed structure shown as a dashed line in Fig. 1(b). In this case, Eqs. (41) are no longer valid. The minimum is sought by means of the Lagrange method as the minimum of the function  $w = g - p(k - l)$  with respect to the variables  $p, k, l$ , where  $p$  is some Lagrange multiplier. The parameters of the first unstable spiral disturbance of the FLL,  $k_0, L_0$  are plotted in Fig. 10. The equality  $k_0 = L_0/d$  holds at almost all fields. That means that the broken vortex chain structure [Fig. 1(b)] presents, in fact, a discrete model of spirals. The pitch length  $L \sim d$  subsiding with the field confirms our hypothesis on the short-wave nature of instability. The value of the critical current of the instability is given then by the formula

$$j_{in} = j_d h_{in}, \quad (43)$$

where the dimensionless current self-field  $h_{in}$  is shown in Fig. 10. The characteristic current of the film,  $j_d = cH_{c1}/2\pi d$ , equals, for the parameters involved,  $j_d = 2.15 \times 10^7$  (A/cm<sup>2</sup>).

Comparing Figs. 10 and 7 one can see that the antiphase mode pitch length  $L_0 \approx 0.6a(h)$  in the considered field region. This result is similar to that for the one-FL mode of the

dense FLL instability in bulk samples obtained by Brandt,<sup>11</sup>  $j_{in} \sim cHa(H)/\lambda^2$ ,  $L_0 \sim 2a(H)$ , where  $a(H) \sim \sqrt{\Phi_0/H}$  is the 2D-lattice spacing.

Let us consider now the uniform mode of the chain instability of the FLL shown in Fig. 9. The upward- and downward-directed vortices occupy the following positions, respectively:

$$\mathbf{R}^+ = (ma + x, 2nL), \quad \mathbf{R}^- = (ma - x, (2n - 1)L), \quad (44)$$

where  $m$  and  $n$  are integer. The distances from the test vortex position at  $\mathbf{R}^+ = (x, 0)$  to the other upward- and downward-directed ones are, respectively,

$$\begin{aligned} \Delta \mathbf{R}^{++}(m, n) &= (ma, 2nL), \\ \Delta \mathbf{R}^{+-}(m, n) &= (ma - 2x, (2n - 1)L). \end{aligned} \quad (45)$$

The energy of this configuration reads

$$\begin{aligned} F &= \frac{1}{aLd} \sum_{m,n} [U_+(\Delta \mathbf{R}^{++}(m, n)) + U_-(\Delta \mathbf{R}^{+-}(m, n))] \\ &= \frac{\varepsilon_0 \pi}{a^2 L^2} \sum_{m,n} \left[ u_+ \left( \frac{2\pi}{a} m, \frac{\pi}{L} n \right) \right. \\ &\quad \left. + u_- \left( \frac{2\pi}{a} m, \frac{\pi}{L} n \right) (-1)^n \cos \left( \frac{4\pi x}{a} m \right) \right]. \end{aligned} \quad (46)$$

Averaging this energy over the distance  $(0, a/2)$  as was done in Eq. (38) one obtains the Gibbs free energy of the uniformly distorted FLL in the form

$$\begin{aligned} g &= -\frac{2\varepsilon_0 k^2}{9ad} + \frac{\varepsilon_0 \sqrt{1+k^2}}{aL} \\ &\quad \times \left\{ \gamma + \ln \frac{L}{\xi} - 2 \ln \left[ 1 + \exp \left( -\frac{\pi a}{L} \sqrt{1+k^2} \right) \right] \right\} \\ &\quad + \frac{\varepsilon_0}{L^2} \left[ \frac{\pi(1+k^2)}{12} - \frac{k^2 a}{2\pi^2 d} \right] - \frac{\pi \varepsilon_0}{6a^2} \left( 1 - \frac{k^2 d^2}{L^2} \right) \\ &\quad - \frac{2\varepsilon_0 kh}{3aL} \ln \frac{d}{2\xi} - \frac{\varepsilon_0 h_i}{2Ld} \ln \frac{\lambda}{\xi}. \end{aligned} \quad (47)$$

The critical values of pitch length, tilt angle, and current triggering the instability may be now found following the same procedure as was used above for the antiphase mode. Though the pictures of the antiphase and uniform modes of instability shown in Figs. 8 and 9 are different as well as the energy expressions (40) and (47), the numerical results for the instability parameters  $k_0$ ,  $L_0$ , and  $h_{in}$  turn out to be almost identical in the considered field region [except for fields very close to  $H_{c1}(d)$ ] thanks to the condition  $k = L/d$  at which the minima are reached.

A typical value of the critical current (43) proportional to  $h_{in}$  (Fig. 10) is very high and exceeds, for example, a characteristic current of a geometrical barrier<sup>33</sup> (or the edge defect current<sup>34</sup>),  $j_b \approx (cH_{c1}/2d) \sqrt{\Lambda/W}$ , by a factor of  $\sqrt{W/\Lambda}$ . It may partly follow from the overestimation of the barrier effect for the vortex chain formation. Really, it is implied in Eqs. (33) and (46) that the energy of the vortex structure at the beginning of the instability process ( $x=0$ ) is rather high.

In fact, the formation of chains occurs not at  $x=0$ , but at some  $x < a/2$  as is seen from Fig. 1(a), which provides less initial energy of the vortex structure. Another point which should be taken into account is the nonuniform distribution of the transport current in a film. Let us suppose that, before instability sets in, the current exhibits a distribution given by Eq. (21). Then, the instability first reveals itself at the edge of the film where the current density is  $\sqrt{W/\Lambda}$  larger than the average one. That means that the instability sets in at the averaged current density  $\sqrt{W/\Lambda}$  less than that of Eq. (43), e.g., at typical currents of the geometrical barrier mechanism.<sup>33</sup> For the parameters of the film chosen in our computations, that gives  $j_{in} \approx 10^5 - 10^6$  A/cm<sup>2</sup>. But anyway, the critical current of instability in thin films under an external field of a few  $H_{c1}(d)$  is high, grows with the magnetic field, and, thus, cannot be matched with the (zero) high-field results obtained for bulk samples in Refs. 10 and 11.

We suppose that the basic reasons for this incompatibility consist in the strong effect of the surface in a thin-film case and in the validity of our straight-vortex model only in the low-field region. Really, the origin of the zero critical current triggering a homogeneous helical instable mode in a bulk case<sup>11</sup> is caused by a very low energy of this mode which is compression free and shear free. In the case of a thin film with  $d \ll \lambda$ , the interaction of the helically distorted FL's with the film surfaces is equivalent to the interaction with a succession of FL reflections<sup>23</sup> in two mirrors located at  $z = \pm d/2$ . This configuration is neither compression free nor shear free and possesses a large energy which results in a large value of the critical current (43). That explains also why the critical currents and parameters of the antiphase and uniform modes of instability in the thin-film case turn out to be so close to each other and to the one-FL mode of FLL instability in the bulk case.<sup>11</sup>

### C. Dissipation cycle frequency and resistivity due to spiral instability of the FLL

Let us estimate the frequency and dissipation rate during the instability-mediated oscillations. Consider a thin film in a parallel field above  $H_{c1}(d)$ . Let the transport current be high enough for an instability to comprise the whole sample. It is reasonable to expect that, in a resistive steady state, the transport current is distributed almost homogeneously over the film.<sup>12,13</sup> Taking into account a threshold character of the instability, the force exerted by the current upon one vortex and averaged over one act of instability may be presented as

$$f = \frac{\Phi_0}{c} (j - j_{in}) d. \quad (48)$$

On the contrary to the above Lorentz force, the viscous force resisting the motion of the vortex is proportional to its length and equals

$$f_\eta = \frac{\eta v d}{\cos \beta}, \quad (49)$$

where  $\beta$  is the angle which the vortex makes with the normal to the film [see Fig. 2(a)] and  $\cos \beta = (1+k^2)^{-1/2}$ . Equating the above two forces one can find an averaged velocity of vortices during the chain expansion:

$$v_{ex} = \frac{f}{\eta} \cos \beta = \frac{c\rho_n(j-j_{in})}{H_{c2}} \cos \beta, \quad (50)$$

where an empirical relation<sup>35</sup> for the viscosity of vortex motion,  $\eta = \Phi_0 H_{c2} / c^2 \rho_n$ , is used,  $\rho_n$  being the resistivity in the normal state.

The characteristic time of recovering a magnetic flux in the sample after the act of instability depends on where the magnetic flux enters. Since the instability current is expected to be of the order or more than the characteristic current of the edge geometrical barrier, it is reasonable to consider the flux entry through the film edges. Then, the downward-directed 2D vortices of the current self-field (tilted in the field direction) enter in the film through the  $x=d/2$  edge and the upward-directed ones enter through the  $x=-d/2$  edge forming the right-handed spiral flux structure similar to right-handed spiral FL's entering the superconducting cylinder.<sup>2</sup> To undergo the reconnection and transformation into additional linear FL's, the entering chains of 2D vortices must pass through a distance  $\sim a(h)$  from the edge to the center of the film. They move with an average velocity

$$v_{en} = \frac{c\rho_n(j-j_b)}{H_{c2}}. \quad (51)$$

Thus, the typical time of the magnetic flux restoration is the same or less than that of flux exit due to the instability. Then, the typical frequency of the shuttling is

$$\begin{aligned} \omega &= \frac{v_{ex}}{a} = \frac{\rho_n c^2 \ln \kappa}{d^2} \frac{h_{in}}{4\kappa^2} \frac{h_{in}}{a/d} \left( \frac{j}{j_{in}} - 1 \right) \cos \beta \\ &= 2.8 \times 10^{11} \text{ (sec}^{-1}\text{)} \frac{h_{in}(h)}{\sqrt{1+k^2(h)} a(h)/d} \left( \frac{j}{j_{in}} - 1 \right) \end{aligned} \quad (52)$$

for the above considered film. The normal resistivity  $\rho_n$ , equal to 100  $\mu\Omega$  cm, was taken for the above estimation from Ref. 29. Let us note that this frequency is current dependent and, thus, a nonuniform current distribution in a film may result in a voltage noise in a wide frequency range.

An averaged electric field in the  $y$  direction generated by the shuttling vortices is proportional to the vortex density in chains and equals

$$E = \frac{\Phi_0 \omega}{cL} \cos \alpha = A \frac{\rho_n \Phi_0 (j-j_{in})}{aLH_{c2} \sqrt{1+k^2}}, \quad (53)$$

where  $\alpha$  is the angle between the magnetic field lines and the normal to the film. As was stressed in Ref. 18, the difference between the  $\alpha$  and the vortex tilt angle  $\beta$  may be drastic in films. Making use of the field expressions (9) one can estimate for the parameters involved an averaged value of  $\cos \alpha$  as  $A \approx 10^{-2}$ . This small value means that the field lines are only slightly deviated from the positions parallel to the film, though the vortices are well tilted to the film surface.

The resistivity during the instability reads

$$\rho_{in} = \frac{E}{j} = \rho_n \left( \frac{\xi}{d} \right)^2 \frac{A2\pi d^2}{aL\sqrt{1+k^2}} \frac{j-j_{in}}{j} \sim 10^{-3} \rho_n \frac{j-j_{in}}{j}. \quad (54)$$

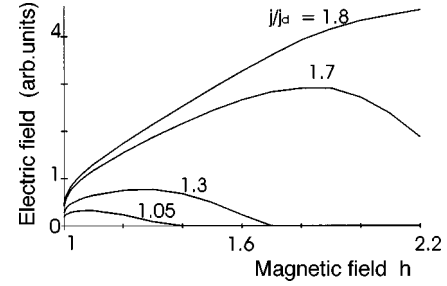


FIG. 11. The electric field  $E$  vs parallel magnetic field  $h = H/H_{c1}(d)$  dependences are presented for fixed values of transport current  $j/j_d = 1.05, 1.3, 1.7, 1.8$ .

Thus, the resistivity due to the instability in thin films has a substantial magnitude. Previous results for the dissipation due to instability were obtained in Refs. 12 and 13 for bulk samples ( $d \gg \lambda$ ) in high fields ( $H \gg H_{c1}$ ) and do not apply directly to our case. Nevertheless, one may use it for the estimation of the resistivity in thin films. The pitch length of the (easiest) uniform mode of instability was found to be infinite, e.g., practically of the length of the sample.<sup>10,11</sup> The resistivity in this regime was found to be<sup>12,13</sup>  $\rho_{in} = 0.2\rho_n(\xi/d)^2$ . It is seen from Eq. (54) taken in the high-current limit  $j \gg j_{in}$  that the short-wave chain instability mechanism in films gives a resistivity one order more than the above long-wave one. This difference is not large, taking into account the model character of our calculations. A much more essential difference is the fact that, in the bulk case, the multiplier  $(\xi/d)^2$  becomes infinitesimally small<sup>12,13</sup> while in the thin-film case this multiplier allows a measurable magnitude of resistivity (54).

The typical current of the spiral instability in thin films (43) is rather high, which makes an observation of the effect difficult but not impossible. At least, the voltage measurements on microbridges and thin narrow films at one order larger currents have been known since the early 1990s.<sup>36</sup> High-quality high- $T_c$  wide thin films with clear-cut edges seem to be appropriate for this experiment too. The homogeneity of the films is important to allow coherent motion of the vortex chains. One possible experiment is a measurement of the voltage at fixed transport currents in a parallel magnetic field near the lower critical field of the film,  $H_{c1}(d)$ . The set of the voltage-magnetic dependences for various values of the transport current  $j$  may be presented in the form  $E$  (V/cm) =  $[B/d^2(\text{nm})] \varphi(j/j_d, h)$  where  $E$  is the electric field strength, the constant  $B = 1.75 \times 10^3$ , and the function  $\varphi(j/j_d, h)$  is shown in Fig. 11. The voltage peak just above the field  $H_{c1}(d)$  is expected in measurements at transport currents  $j \approx j_d$ . The decrease of the voltage may be, though, difficult to observe since the large heat release after the onset of instability will most likely trigger a global irreversible quench of the superconducting state.

Another possibility to reveal the indications of the spiral instability is given by local magnetic measurements. In the inner region of the film, the  $z$  components of the magnetic moments of the 2D vortices with opposite orientations compensate for each other and make no contribution in a field transverse to the film. But in the narrow strip of the width  $\sim d$  along the film edges, the chain instability induces the oscillating transverse field of the amplitude  $H$

$\sim(\Phi_0/aL)\cos\alpha\approx 10^{-2}T$  (for the parameters chosen) and of the frequency given in Eq. (52). The detection of this field component perpendicular to the film seems to be possible in films with a clear-cut edge and would be a strong evidence in favor of the suggested scenario of resistivity in a parallel field.

#### IV. CONCLUSIONS

In this paper we have presented a discrete model of a resistive state in thin superconducting films carrying a transport current parallel to an external field direction.

A one-dimensional flux-line lattice existing in a field region above the lower critical field is shown to be unstable against certain regular distortions similar to the left-handed spiral instability of force-free configurations in bulk superconductors. If the transport current density is high enough, every linear flux line transforms into a double chain of 2D vortices tilted in the field direction and forming a left-spiral-like flux structure. These double chains expand, driven by the transport current, reconnect, and form a new one-dimensional flux-line lattice, allowing a part of flux to leave the sample. Finally, the equilibrium flux magnitude in the sample recovers due to the entry of additional flux lines through the edges of the sample.

The critical current triggering the instability is of the order or above the characteristic current of the geometrical barrier. Thanks to the high current and a short pitch length of the instable flux structures, the typical frequency of the above shuttle process is rather high (about  $10^{11}$  sec $^{-1}$ ) and strongly current dependent. If the transport current is distrib-

uted nonuniformly over the sample [to, say, after the law (21)], vortex shuttling may give rise to a voltage noise spectrum in a rather wide frequency range of many decades that makes difficult an observation of a distinct oscillation effect. Nevertheless, the observation of the transverse component of the magnetic field at the clear-cut film edge would be an evidence in favor of the proposed chain instability mechanism of resistivity which gives a quite reasonable magnitude of the dissipation rate.

#### ACKNOWLEDGMENTS

The authors are indebted to Dr. E. H. Brandt and Professor J. R. Clem, Professor A. Campbell, and Professor V. K. Vlasko-Vlasov for a useful discussion of the results. Yu.A.G. would like to acknowledge the support of this work by the Alexander von Humboldt Foundation and the kind hospitality at the Material Physics Institute of the University of Göttingen.

#### APPENDIX: INTERACTION ENERGY OF THE TILTED VORTICES

Substituting Eqs. (9) and (10) into Eq. (12) one obtains Eq. (13) with

$$u_+(\mathbf{q}) = \frac{1+k^2}{Q^2+(\mathbf{k}\cdot\mathbf{q})^2} + \frac{2}{(Q^2+(\mathbf{k}\cdot\mathbf{q})^2)^2 d} \Pi_+, \quad (\text{A1})$$

$$u_-(\mathbf{q}) = -\frac{1-k^2}{Q^2+(\mathbf{k}\cdot\mathbf{q})^2} \frac{\sin(\mathbf{k}\cdot\mathbf{q}d)}{(\mathbf{k}\cdot\mathbf{q}d)} + \frac{2}{(Q^2+(\mathbf{k}\cdot\mathbf{q})^2)^2 d} \Pi_-, \quad (\text{A2})$$

where

$$\begin{aligned} \Pi_{\pm}(\mathbf{q}) = & (\mathbf{k}\cdot\mathbf{q})(Q \cosh Qd + q \sinh Qd) \left[ \pm \frac{Q \cos \mathbf{k}\cdot\mathbf{q}d/2 \sinh Qd/2 + \mathbf{k}\cdot\mathbf{q} \sin \mathbf{k}\cdot\mathbf{q}d/2 \cosh Qd/2}{(Q \sinh Qd/2 + q \cosh Qd/2)^2 \sinh Qd/2} \sin \mathbf{k}\cdot\mathbf{q}d/2 \right. \\ & \left. - \frac{Q \sin \mathbf{k}\cdot\mathbf{q}d/2 \cosh Qd/2 - \mathbf{k}\cdot\mathbf{q} \cos \mathbf{k}\cdot\mathbf{q}d/2 \sinh Qd/2}{(Q \cosh Qd/2 + q \sinh Qd/2)^2 \cosh Qd/2} \cos \mathbf{k}\cdot\mathbf{q}d/2 \right] \\ & + \frac{Q \sin \mathbf{k}\cdot\mathbf{q}d/2 \cosh Qd/2 - \mathbf{k}\cdot\mathbf{q} \cos \mathbf{k}\cdot\mathbf{q}d/2 \sinh Qd/2}{\lambda^2 (Q \cosh Qd/2 + q \sinh Qd/2)^2} \sinh Qd/2 \sin \mathbf{k}\cdot\mathbf{q}d/2 \\ & \pm \frac{Q \cos \mathbf{k}\cdot\mathbf{q}d/2 \sinh Qd/2 + \mathbf{k}\cdot\mathbf{q} \sin \mathbf{k}\cdot\mathbf{q}d/2 \cosh Qd/2}{\lambda^2 (Q \sinh Qd/2 + q \cosh Qd/2)^2} \cosh Qd/2 \cos \mathbf{k}\cdot\mathbf{q}d/2 \\ & - k^2 \left[ Q \left( \frac{\sinh Qd/2}{\cosh Qd/2} \cos^2 \mathbf{k}\cdot\mathbf{q}d/2 \pm \frac{\cosh Qd/2}{\sinh Qd/2} \sin^2 \mathbf{k}\cdot\mathbf{q}d/2 \right) + \frac{(1\mp 1)}{2} (\mathbf{k}\cdot\mathbf{q}) \sin \mathbf{k}\cdot\mathbf{q}d \right]. \quad (\text{A3}) \end{aligned}$$

Equations (16) follow from the above expressions (A1)–(A3) in the limit  $|q_y|d = \pi nd/L \gg 1$ . The second terms in both equations (16) make essential contributions only in the region  $qd < 1$  and are cut off for convenience (at  $qd > 1$  they decrease much faster).

Equations (35) may be found from Eqs. (A1)–(A3) in the limit  $q = q_{m,n} \gg d^{-1}$  valid for any  $m \neq 0$  or  $n \neq 0$  since  $q_{m,n} = (\pi m/a, \pi n/L)$  and  $a, L < d$ . Then, the terms making the main contribution in sums (34) and (46) are saved.

- <sup>1</sup>E. H. Brandt, Rep. Prog. Phys. **58**, 1465 (1995).
- <sup>2</sup>A. M. Campbell and J. E. Evetts, *Critical Currents in Superconductors* (Taylor & Francis, London, 1972).
- <sup>3</sup>K. Kadowaki, Y. Songliu, and K. Kitazawa, Supercond. Sci. Technol. **7**, 519 (1994); G. E. Marsh, Phys. Rev. B **50**, 571 (1994); M. Shvartsner, M. Gitterman, and B. Ya. Shapiro, Physica C **264**, 204 (1996); T. J. Hagenaars, E. H. Brandt, R. E. Hetzel, W. Hanke, M. Leghissa, and G. Saemann-Ischenko, Phys. Rev. B **55**, 11 706 (1997); T. J. Hagenaars and E. H. Brandt, *ibid.* **56**, 11 435 (1997); E. A. Jagla, *ibid.* **57**, 5466 (1998).
- <sup>4</sup>M. A. R. LeBlanc, S. Celebi, S. X. Wang, and V. Plecháček, Phys. Rev. Lett. **71**, 3367 (1993); S. J. Park and J. S. Kouvel, Phys. Rev. B **48**, 13 995 (1993).
- <sup>5</sup>I. L. Landau, Zh. Éksp. Teor. Fiz. **64**, 557 (1973) [Sov. Phys. JETP **37**, 2851 (1973)].
- <sup>6</sup>D. G. Walmsley and W. E. Timms, J. Phys. F **7**, 2373 (1977).
- <sup>7</sup>T. S. Teasdale and H. E. Rorschach, Phys. Rev. **90**, 709 (1953).
- <sup>8</sup>J. R. Clem, Phys. Lett. **54A**, 452 (1975).
- <sup>9</sup>J. R. Clem, Phys. Rev. Lett. **38**, 1425 (1977).
- <sup>10</sup>E. H. Brandt, Phys. Lett. **79A**, 207 (1980); Phys. Rev. B **25**, 5756 (1982).
- <sup>11</sup>E. H. Brandt, J. Low Temp. Phys. **44**, 33 (1981); **44**, 59 (1981).
- <sup>12</sup>J. R. Clem, J. Low Temp. Phys. **38**, 353 (1980).
- <sup>13</sup>E. H. Brandt, J. Low Temp. Phys. **39**, 41 (1980).
- <sup>14</sup>A. A. Abrikosov, Zh. Éksp. Teor. Fiz. **46**, 1464 (1964) [Sov. Phys. JETP **19**, 988 (1964)].
- <sup>15</sup>V. V. Shmidt, Zh. Éksp. Teor. Fiz. **57**, 2095 (1969) [Sov. Phys. JETP **30**, 1137 (1969)]; **61**, 398 (1971) [**34**, 211 (1972)].
- <sup>16</sup>A. I. Rusinov and G. S. Mkrtchyan, Zh. Éksp. Teor. Fiz. **61**, 773 (1971) [Sov. Phys. JETP **34**, 413 (1972)].
- <sup>17</sup>Yu. A. Genenko, Phys. Rev. B **53**, 11 757 (1996).
- <sup>18</sup>E. H. Brandt, Phys. Rev. B **48**, 6699 (1993).
- <sup>19</sup>A. Yu. Martynovich, Zh. Éksp. Teor. Fiz. **105**, 912 (1994) [JETP **78**, 489 (1994)].
- <sup>20</sup>R. S. Thompson, Sov. Phys. JETP **42**, 1144 (1975).
- <sup>21</sup>E. V. Minenko and I. O. Kulik, Sov. J. Low Temp. Phys. **5**, 583 (1979).
- <sup>22</sup>J. Pearl, Appl. Phys. Lett. **5**, 65 (1964).
- <sup>23</sup>E. H. Brandt, J. Low Temp. Phys. **42**, 557 (1981).
- <sup>24</sup>V. G. Kogan, A. Yu. Simonov, and M. Ledvij, Phys. Rev. B **48**, 392 (1993).
- <sup>25</sup>Yu. M. Ivanchenko, A. I. Kozinskaja, and Yu. V. Medvedev, Sov. Phys. Solid State **21**, 1989 (1979).
- <sup>26</sup>P. de Gennes, *Superconductivity in Metals and Alloys* (Benjamin, New York, 1966).
- <sup>27</sup>J. R. Clem, R. P. Huebener, and D. E. Gallus, J. Low Temp. Phys. **12**, 449 (1973).
- <sup>28</sup>A. I. Larkin and Yu. N. Ovchinnikov, Zh. Éksp. Teor. Fiz. **61**, 1221 (1971) [Sov. Phys. JETP **34**, 651 (1972)].
- <sup>29</sup>M. N. Kunchur, D. K. Christen, and J. M. Phillips, Phys. Rev. Lett. **70**, 998 (1993).
- <sup>30</sup>N. Ya. Fogel and V. G. Cherkasova, Physica B **107**, 291 (1981).
- <sup>31</sup>G. Carneiro, Phys. Rev. B **57**, 6077 (1998).
- <sup>32</sup>Yu. A. Genenko, Phys. Rev. B **51**, 3686 (1995).
- <sup>33</sup>M. V. Indenbom, H. Kronmüller, T. W. Li, P. H. Kes, and A. A. Menovsky, Physica C **222**, 203 (1994); E. Zeldov, A. I. Larkin, V. B. Geshkenbein, M. Konczykowski, D. Majer, B. Khaykovich, V. M. Vinokur, and H. Shtrikman, Phys. Rev. Lett. **73**, 1428 (1994).
- <sup>34</sup>M. Yu. Kupriyanov and K. K. Likharev, Sov. Phys. Solid State **16**, 1835 (1975).
- <sup>35</sup>Y. B. Kim, C. F. Hempstead, and A. R. Strnad, Phys. Rev. **139**, A1163 (1965).
- <sup>36</sup>S. Tahara, S. M. Anlage, J. Halbritter, C. B. Eom, D. K. Fork, T. H. Geballe, and M. R. Beasley, Phys. Rev. B **41**, 11 203 (1990); H. Jiang, Y. Huang, H. How, S. Zhang, C. Vittoria, A. Widom, D. B. Chrisey, J. S. Horwitz, and R. Lee, Phys. Rev. Lett. **66**, 1785 (1991); I. Zaquine, G. Ben Assayaq, J. Gierak, B. Desertene, B. Marcilhac, M. Mercandalli, and J. C. Mage, J. Appl. Phys. **72**, 270 (1992).